

Electronic structure of 3°-twisted bilayer graphene on 4H-SiC(0001)

Takushi Iimori ¹, Anton Visikovskiy,² Hitoshi Imamura ², Toshio Miyamachi,¹ Miho Kitamura,^{3,4} Koji Horiba,^{3,4} Hiroshi Kumigashira,^{3,5} Kazuhiko Mase,^{3,4} Kan Nakatsuji,⁶ Satoru Tanaka,² and Fumio Komori ^{1,*}

¹*Institute for Solid State Physics, The University of Tokyo, Kashiwa, Chiba 277-8581, Japan*

²*Department of Applied Quantum Physics and Nuclear Engineering, Kyushu University, Fukuoka 819-0395, Japan*

³*Institute of Materials Structure Science, High Energy Accelerator Research Organization (KEK), Tsukuba 305-0801, Japan*

⁴*Department of Materials Structure Science, SOKENDAI (The Graduate University for Advanced Studies), Tsukuba 305-0801, Japan*

⁵*Institute of Multidisciplinary Research for Advanced Materials (IMRAM), Tohoku University, Sendai 980-8577, Japan*

⁶*Department of Materials Science and Engineering, Tokyo Institute of Technology, Yokohama 226-8502, Japan*



(Received 11 February 2021; accepted 21 April 2021; published 13 May 2021)

The electronic structure of 3°-twisted bilayer graphene (TBG) is studied by angle-resolved photoelectron spectroscopy (ARPES). Sub-mm-sized TBG prepared by direct bonding in a high vacuum enabled us to use conventional ARPES band mapping with synchrotron light. The results indicate that strong interlayer coupling makes a moiré potential for the Dirac electrons and significantly modifies the graphene bands around the \bar{K} points such as the band splitting and electron velocity reduction. The observed electronic structure is consistently reproduced by tight-binding calculations combined with a band unfolding method.

DOI: [10.1103/PhysRevMaterials.5.L051001](https://doi.org/10.1103/PhysRevMaterials.5.L051001)

Moiré superlattices made by stacking two-dimensional (2D) monolayers have been studied as systems with novel electronic structures. In particular, twisted bilayer graphene (TBG) has attracted much attention for more than a decade because the interlayer interaction largely modifies the band structure from that of single-layer graphene, depending on the twisting angle θ [1–3]. Interesting electronic properties, such as chirality [4], superconductivity [5], ferromagnetism [6], and the quantum anomalous Hall effect [7] have been discussed both theoretically and experimentally [8–10]. As an experimental study of the electronic states, van Hove singularity (vHs) in the density of states, which is associated with the formation of flat bands and gaps, was investigated using scanning tunneling microscopy/spectroscopy [11–13] and magnetotransport [14,15]. The renormalization of the band velocity near the Dirac energy was found by Landau level spectroscopy [16,17]. The observed energy positions of vHs and the velocity reduction consistently depend on θ in some experiments while they were absent in some other samples. It was pointed out that the band renormalization appears only in a sample with strong interlayer coupling [17].

The band structure of TBG has been directly measured using angle-resolved photoelectron spectroscopy (ARPES). The presence of vHs at the point of the crossing two Dirac cones was clarified for samples with θ between 5° and 30° [18–20]. With decreasing θ , flat bands can partially evolve at the energy of vHs, and the velocity at the Dirac point is reduced. These will turn to wide flat bands in the TBG with θ around 1° [5]. Recently, flat bands for samples with θ around 1° have been reported [21,22]. However, the modified band structure including the velocity reduction for a few-degree

rotated TBG has not been reported two-dimensionally except in Refs. [21,22]. The substrate-graphene interaction was again suggested as the origin of the absence of the velocity reduction for 2.1° TBG [23].

In the present Letter, we show the detailed band structure of a 3.2° TBG studied by ARPES with conventional hemispherical spectrometers and synchrotron light. Here, we use the sample made by direct bonding in a vacuum after *in situ* cleaning the graphene surface for minimizing the interface impurity between the graphene layers [24]. The interlayer coupling in the present sample is strong enough to renormalize the band structure. Our two-dimensional band mapping demonstrates the band modification in the wave-number space near the two \bar{K} points of the upper and lower graphene layers. The results are well reproduced by the electronic structure calculated by tight-binding and band unfolding methods [25].

The detailed method of our TBG fabrication was given in Ref. [24]. We used single-layer graphene on a Si-terminated surface of nitrogen-doped 4H-SiC(0001) substrates prepared by chemical vapor deposition with oxygen. Here, there is an interface layer with a 3×3 superstructure between graphene and the substrate SiC(0001). The two substrates with single-layer graphene were placed in a high vacuum chamber facing each other, and the following fabrication process was done in a vacuum of about 1×10^{-4} Pa. First, the relative crystal orientations of the two sheets were adjusted using reflection high-energy electron diffraction. Here, the angle alignment error was about $\pm 4^\circ$. Then, they were annealed at 200 °C for cleaning the surface. With keeping the same temperature, the two substrates were once pressed together face to face up to 6×10^6 Pa, and finally parts of graphene on the one substrate are peeled off onto graphene on the other substrate. Consequently, three areas with TBG, with monolayer graphene, and without graphene coexist in the present substrate. It is

*komori@issp.u-tokyo.ac.jp

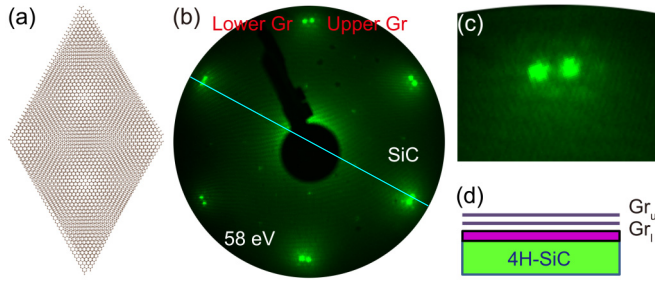


FIG. 1. (a) Schematic illustration of 3° TBG. (b) LEED image of the 3.2° TBG sample at 58 eV electron energy. The spots from both lower and upper graphene (Gr) layers are separately seen. The light blue line connects the spots from the lower graphene and interface 3×3 superstructure. (c) Magnified graphene LEED image of the same TBG sample indicating satellite spots due to the moiré superstructure. (d) Schematic structure model of the TBG (upper-layer graphene Gr_u and lower Gr_l). The purple part between Gr_l and the 4H-SiC substrate represents the interface layer with a 3×3 superstructure.

noted that the interface layer with the 3×3 superstructure is more weakly bonded to the surface graphene than the usual $(6\sqrt{3} \times 6\sqrt{3})R30^\circ$ carbon interface layer [26] of the thermally decomposed graphene on SiC(0001). Thus, the present graphene is easily peeled off from the substrate.

The formation of TBG areas was confirmed by μ -Raman spectroscopy and low-energy electron diffraction (LEED). Figures 1(b) and 1(c) show the LEED patterns of a TBG sample. The spots from the two graphene sheets, the interface 3×3 superstructure, and SiC substrate are seen with satellite spots due to the TBG moiré structure. By analyzing the interval of the satellite spots [24], the twist angle θ is estimated to be $3.2 \pm 0.3^\circ$. In the present Letter, we focus on this sample.

The electronic structure was studied using ARPES with linearly polarized synchrotron light at room temperature (RT) in BL-13B [27] and at 30 K in BL-2A of the Photon Factory, KEK. The beam sizes at the sample and photon energy were $50 \times 300 \mu\text{m}^2$ and 52 eV in BL-13B, and $100 \times 500 \mu\text{m}^2$ and 42 eV in BL-2A. Before the LEED observations and ARPES measurements, the graphene surface was cleaned by annealing at 700 K for 30 min in a vacuum better than 5×10^{-10} Torr. The graphene and interface 3×3 superstructure were confirmed by LEED before the ARPES measurements. In the measurements, we selected the area of the sample with high ARPES intensity from the upper-layer graphene.

A tight-binding method with a periodicity-free unfolding approach [25] was used for the band calculation of TBG. We made a free-standing and commensurate periodic model of the twist angle 3.14° with 1324 carbon atoms for the present sample. The spectral weight is calculated as a function of the wave vector in this method, and compared with the results of ARPES band mapping [28].

In Fig. 2(a), we show the constant-energy band mapping at a Fermi energy E_F around the two \bar{K} points, the upper-layer \bar{K}_u and lower-layer \bar{K}_l [see Figs. 2(d) and 2(e) for the graphene Brillouin zone (BZ) and for moiré BZ], and the ARPES band image along the line through \bar{K}_u and \bar{K}_l [28]. The data were obtained at RT, and the origin of the binding energy is E_F . In

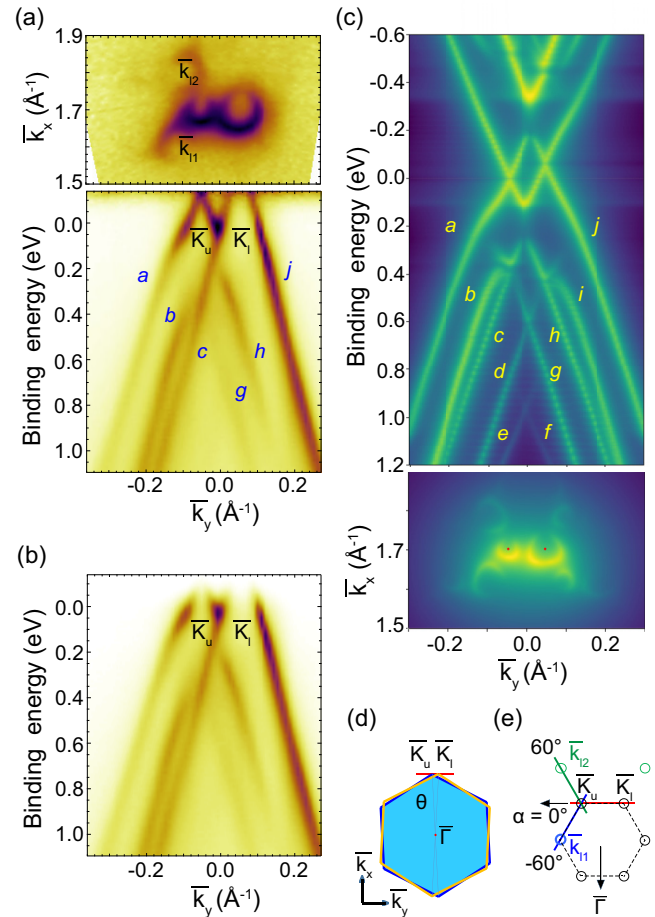


FIG. 2. (a) ARPES constant-energy band image at E_F (upper) and (lower) ARPES band dispersion image along the line through the two \bar{K} points, \bar{K}_u (upper layer) and \bar{K}_l (lower layer). The data were taken at RT. The logarithmic ARPES intensity is displayed in the upper figure for showing replica bands clearly, and the linear intensity in the lower. Replica \bar{K}_l points are shown as \bar{k}_{l1} and \bar{k}_{l2} . (b) ARPES band dispersion image without the division by the Fermi-Dirac distribution curve along the same line as in (a). (c) Calculated band structure of TBG with $\theta = 3.14^\circ$ (upper). The energy difference between the upper and lower graphene layers is set to be 0.05 eV. The band intensity indicates the calculated spectral weight, and the logarithmic intensity is displayed. Calculated constant-energy band image of TBG with $\theta = 3.14^\circ$ at 0.08 eV below E_F (lower). The logarithmic intensity is displayed. The left and right red dots indicate \bar{K}_u and \bar{K}_l , respectively. (d) Graphene BZ and (e) moiré BZ for TBG. \bar{k}_{l1} and \bar{k}_{l2} are \bar{K} points of the replica lower graphene Dirac bands adjacent to the original upper graphene Dirac band. Definition of the angle α around \bar{K}_u is given in (e).

the upper image, the replica \bar{K}_l bands, \bar{k}_{l1} and \bar{k}_{l2} , are seen around the \bar{K}_u point. In the band image, the ARPES intensity was divided by the Fermi-Dirac distribution curve for making the band structure above E_F clear. The band image without the division by the Fermi-Dirac distribution curve is shown in Fig. 2(b). It is noted that the ARPES intensity from the region without the upper-layer graphene overlaps with that from the lower layer of TBG in the images.

Both graphene layers are positively (p) doped, i.e., each Dirac energy E_D is higher than E_F , and the doping level is

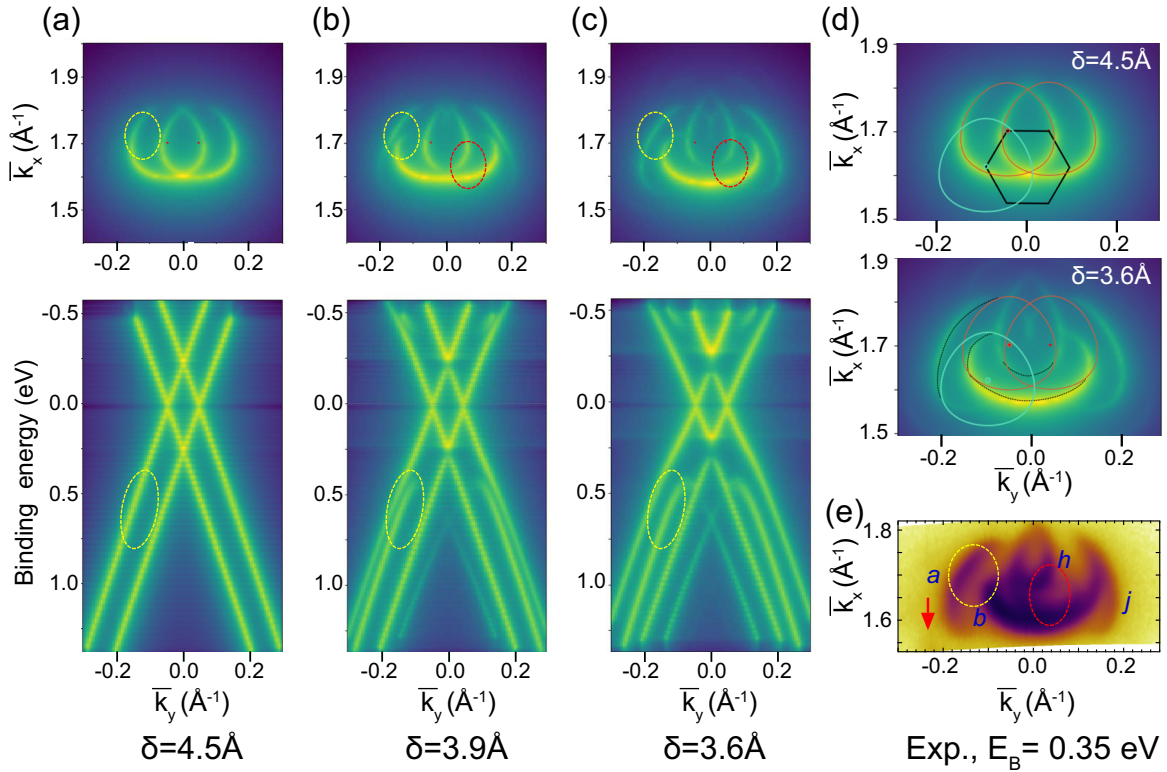


FIG. 3. (a)–(c) The calculated band structure of the 3.14° TBG. In each panel, the upper figure indicates the constant-energy map at $E = E_F - 0.6$ eV, and the lower one the dispersion along the line through \bar{K}_u and \bar{K}_l . Here, both graphene layers have the same E_D , which is equal to E_F . The interlayer spacing δ is 4.5, 3.9, and 3.6 Å. The logarithmic intensity is displayed. Yellow and red dotted ovals indicate the positions of the band splitting, and red dots the positions of \bar{K}_u and \bar{K}_l . (d) Constant-energy maps for $\delta = 4.5$ Å (upper) and 3.6 Å (lower) with the two original Dirac bands (red curves) and replica band (light blue curve). Red dots indicate the positions of \bar{K}_u and \bar{K}_l , and the light-blue dot the position of the replica \bar{K}_l point. The black hexagon in the upper panel is the moiré BZ, and the black dotted curves in the lower panel indicate the split bands. (e) Observed constant-energy ARPES intensity map at 0.35 eV below E_F . The data were taken at 30 K, and the logarithmic intensity is displayed. The intensity marked as a , b , h , and j originates from the corresponding bands shown in Fig. 2(b). The red arrow indicates the intensity due to a replica band.

higher in the lower layer than in the upper one. Single-layer graphene on the present 3×3 interface layer is p doped in contrast to negatively doped graphene on the thermally decomposed $(6\sqrt{3} \times 6\sqrt{3})R30^\circ$ carbon interface layer. The doping level of graphene on substrates depends on the interface electronic structure. However, the atomic and electronic structures of the 3×3 interface have not been clarified yet. Thus, the origin of the p doping is unknown at present.

The calculated band structure of the 3.14° TBG is shown in the upper panel of Fig. 2(c). Here, Dirac energies of the upper and lower graphene are set to be 0 and 0.05 eV above E_F by considering the observed difference shown in Fig. 2(a), and the interlayer distance to be 3.44 Å for reproducing the experimental results (see the discussion below). This value is a little larger than the experimentally determined interlayer distance of the normal bilayer graphene on SiC(0001), 3.35 Å [29].

Ten bands are recognized in the figure as a – j . By comparing the ARPES band image shown in Fig. 2(a) with the calculated band structure, the bands a , b , c , g , h , and j correspond to the observed bands as marked in Fig. 2(a). In particular, the observed bands a , b , g and h , which originate from the upper TBG band, exhibit a significant difference

from the original Dirac linear bands. The bands a and b (i and j) are split from the original upper-layer (lower-layer) graphene band owing to the band crossing to the adjacent replica Dirac band. The observed linear bands c and j in Fig. 2(a) are attributed to the dominant ARPES intensity from the coexisting single-layer graphene, i.e., without the upper layer, in the measurement area. In other words, the ARPES intensity from the lower TBG bands in the sample was weaker than that from the single-layer graphene, and they overlap with each other.

In the lower panel of Fig. 2(c), we show the calculated constant-energy band image at 0.08 eV below E_F . This image corresponds to the experimental data shown in the upper panel of Fig. 2(a). Replica bands are well reproduced in the calculation.

We demonstrate the band change due to the interlayer coupling of TBG theoretically in Figs. 3(a)–3(c). Here, the doping difference is not considered for simplicity. For weakly coupled TBG, two overlapping Dirac cones just appear as in the upper panels of Figs. 3(a) and 3(d). With the decrease of the interlayer distance δ , i.e., the increase of the interlayer coupling, the band b splits from the band a as the area marked by yellow dotted ovals in Figs. 3(b) and 3(c), and the

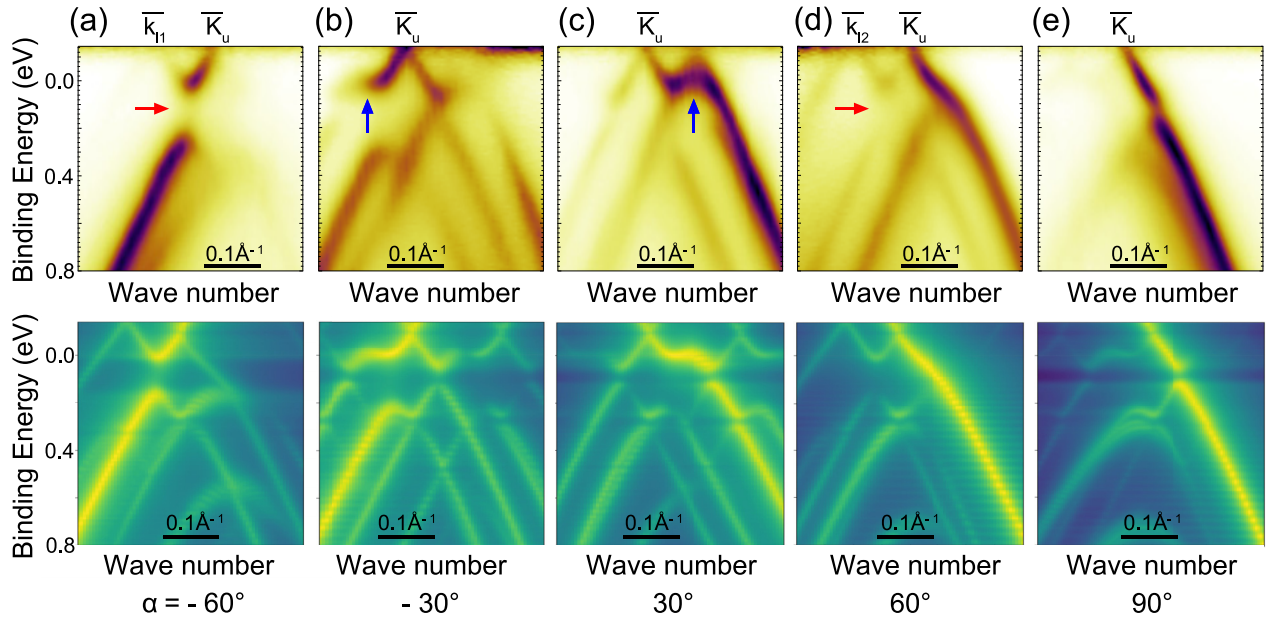


FIG. 4. Observed (upper) and calculated (lower) band images in the five planes rotated around \bar{K}_u . The rotation angle α is defined as an angle from the \bar{K}_u - \bar{K}_l line as given in Fig. 2(d). The spectra were taken at RT and the ARPES intensity was divided by the Fermi-Dirac distribution curve. The data without division by the Fermi-Dirac distribution curve are given in Ref. [28]. Red arrows indicate the positions of the energy gap (a) between \bar{K}_u and \bar{k}_{l1} and (d) between \bar{K}_u and \bar{k}_{l2} , and blue arrows in (b) and (c) the partial flat bands.

dispersion of the band *a* deviates from the linear one for $\delta = 3.6 \text{ \AA}$. This is due to band repulsion between the original and replica cones. The band splits in the other areas in the wave-number space as in the area marked by red dotted ovals in Figs. 3(b) and 3(c), and the black dotted curves in the lower panel of Fig. 3(d).

The band modifications from the original trigonally warped Dirac bands in Fig. 3(c) were consistently observed in the upper graphene bands as in the marked areas in the constant-energy ARPES map shown in Fig. 3(e). Here, the result at 30 K is shown. The modified upper bands, *a*, *b*, and *h* have almost the same shapes in the constant-energy map as in the calculation. The ARPES intensity from the modified lower graphene band *j* is weak in Fig. 3(e) compared with the intensity from the single-layer graphene, which coexists with TBG on the substrate. Parts of the modified replica bands were also observed consistently with the results of the calculation [28]. The red arrow in Fig. 3(e) indicates an example of the intensity from the replica band.

In the experiment, the hybridization energy gap between \bar{K}_u and \bar{K}_l was observed for the band *h* at $\bar{k}_y = 0.0 \text{ \AA}^{-1}$ and $E = 0.1 \text{ eV}$ below E_F in Fig. 2(a). The gap in the band *c* was not observed at $\bar{k}_y = 0.0 \text{ \AA}^{-1}$ because of the strong ARPES intensity from the single-layer graphene. The same band gap was clearly observed in the band image along the line between \bar{K}_u and the replica \bar{K} point, \bar{k}_{l1} , as shown in Fig. 4(a). The replica band is not concealed by the ARPES intensity from the area of the single-layer graphene. The same gap can be seen in the band image along the line between \bar{K}_u and the other replica \bar{K} point, \bar{k}_{l2} , as in Fig. 4(d). The size of the energy gap of the band *h* is $0.24 \pm 0.03 \text{ eV}$, which was estimated by the energy distribution curve [28], and is the same as that of the 4° TBG made by the same method [24] within the experimental accuracy.

The band structures in the other three directions around \bar{K}_u for $\alpha = -30^\circ, 30^\circ$, and 90° are also shown in Fig. 4 with the calculated band structure. Here, the angle α around \bar{K}_u is defined from the \bar{K}_u - \bar{K}_l line as in Fig. 2(e). The qualitative features of the observed TBG band map are well reproduced by the tight-binding calculation, such as the flat-band features near E_F for $\alpha = \pm 30^\circ$ and the various energy gaps [28]. The partial flat band appears around the position of vHs, that is, the point of the two crossing Dirac cones. It will develop further with decreasing the twisted angle, and eventually turn into a wide flat band at the magic angle [5,21,22]. The evolution of the flat-band feature is demonstrated in the present study while the saddle-point features of vHs were reported in previous reports for $\theta \geq 5^\circ$ [18–20].

There are quantitative discrepancies in the details of the band shapes between the results of the experiments and calculations. For example, the dispersion of the calculated band *a* in Fig. 2(b) deviates more strongly from the linear one than in the experimental result. Quantitative discrepancies can be attributed to our simple structural model of TBG. It was theoretically pointed out that the honeycomb carbon lattice of a few-degree rotated TBG distorts for making the *AB* stacking area wider with three-dimensional local lattice distortion than that in the simple stacking [30–33]. The interlayer coupling largely depends on the local stacking and interlayer lattice distance, and the lattice distortion would cause modifications of the band structure in TBG differently from those expected from the simple moiré structure as given in these references. Further band calculations for the optimized lattice structure are necessary for a quantitative discussion.

In the present sample, TBG is *p* doped, and the flat-band features appear near E_F by chance. When we change the rotation angle, the position of the flat band will be apart from

E_F . However, it is possible to tune the flat-band energy by doping with adsorbates and/or by using single-layer graphene on the other substrate as the lower layer. It would be even possible to fabricate a device of the present TBG with gates for continuous tuning of the E_F position. These will open the way to study and tune the electron correlation in the flat bands, such as the band-gap opening.

In summary, we have studied the electronic structure of a wide 3.2° TBG made by exfoliation in a vacuum with a clean interface using the ARPES band mapping, and demonstrated the modification of the band structure in two-dimensional wave-number space. The experimental results indicate anisotropic band dispersion around the Dirac energy, and the formation of local flat bands in the wave-number space. All these features are consistent with the results of the tight-binding calculations using the unfolding method. A combination of a wide sample with a clean interface and a

quantitative evaluation by ARPES provides a useful way for understanding the electronic states of artificially stacked 2D materials.

We thank Yu-ichiro Matsushita and Atsushi Oshiyama for valuable discussions on the tight-binding calculations and the experimental results. We also thank Iwao Matsuda and Suguru Ito for collaborations in the ARPES measurements, and Ryu Yukawa, Yukiaki Ishida, and Koichiro Yaji for the ARPES data analyses. This work was partly supported by JSPS Grant-in-Aid for Scientific Research (B), KAKENHI, Grants No. JP18H01146 and No. JP19H02595; for Scientific Research on Innovative Areas Grant No. 20H05179; for Challenging Research (Exploratory) Grant No. JP20K21119. The ARPES measurements were performed at BL-13B and BL-2A, Photon Factory, KEK, Japan (PF-PAC Grants No. 2017G575 and No. 2019G632).

-
- [1] J. M. B. Lopes dos Santos, N. M. R. Peres, and A. H. Castro Neto, Graphene Bilayer with a Twist: Electronic Structure, *Phys. Rev. Lett.* **99**, 256802 (2007).
- [2] R. Bistritzer and A. H. MacDonald, Moiré bands in twisted double-layer graphene, *Proc. Natl. Acad. Sci. U.S.A.* **108**, 12233 (2011).
- [3] J. M. B. Lopes dos Santos, N. M. R. Peres, and A. H. Castro Neto, Continuum model of the twisted graphene bilayer, *Phys. Rev. B* **86**, 155449 (2012).
- [4] C.-J. Kim, A. Sanchez-Castillo, Z. Ziegler, Y. Ogawa, C. Noguez, and J. Park, Chiral atomically thin films, *Nat. Nanotechnol.* **11**, 520 (2016).
- [5] Y. Cao, V. Fatemi, S. Fang, K. Watanabe, T. Taniguchi, E. Kaxiras, and P. Jarillo-Herrero, Unconventional superconductivity in magic-angle graphene superlattices, *Nature (London)* **556**, 43 (2018).
- [6] A. L. Sharpe, E. J. Fox, A. W. Barnard, J. Finney, K. Watanabe, T. Taniguchi, M. A. Kastner, and D. Goldhaber-Gordon, Emergent ferromagnetism near three-quarters filling in twisted bilayer graphene, *Science* **365**, 605 (2019).
- [7] M. Serlin, C. L. Tschirhart, H. Polshyn, Y. Zhang, J. Zhu, K. Watanabe, T. Taniguchi, L. Balents, and A. F. Young, Intrinsic quantized anomalous Hall effect in a moiré heterostructure, *Science* **367**, 900 (2020).
- [8] A. Rozhkov, A. Sboychakov, A. Rakhmanov, and F. Nori, Electronic properties of graphene-based bilayer systems, *Phys. Rep.* **648**, 1 (2016).
- [9] S. Carr, S. Fang, and E. Kaxiras, Electronic-structure methods for twisted moire layers, *Nat. Rev. Mater.* **5**, 748 (2020).
- [10] G. Abbas, Y. Li, H. Wang, W.-X. Zhang, C. Wang, and H. Zhang, Recent advances in twisted structures of flatland materials and crafting moire superlattices, *Adv. Func. Mater.* **30**, 2000878 (2020).
- [11] Z. Ni, Y. Wang, T. Yu, Y. You, and Z. Shen, Reduction of Fermi velocity in folded graphene observed by resonance raman spectroscopy, *Phys. Rev. B* **77**, 235403 (2008).
- [12] G. Li, A. Luican, J. M. B. Lopes dos Santos, A. H. Castro Neto, A. Reina, J. Kong, and E. Y. Andrei, Observation of van Hove singularities in twisted graphene layers, *Nat. Phys.* **6**, 109 (2010).
- [13] I. Brihuega, P. Mallet, H. González-Herrero, G. Trambly de Laissardière, M. M. Ugeda, L. Magaud, J. M. Gómez-Rodríguez, F. Ynduráin, and J.-Y. Veuillen, Unraveling the Intrinsic and Robust Nature of van Hove Singularities in Twisted Bilayer Graphene by Scanning Tunneling Microscopy and Theoretical Analysis, *Phys. Rev. Lett.* **109**, 196802 (2012).
- [14] Y. Kim, P. Herlinger, P. Moon, M. Koshino, T. Taniguchi, K. Watanabe, and J. H. Smet, Charge inversion and topological phase transition at a twist angle induced van Hove singularity of bilayer graphene, *Nano Lett.* **16**, 5053 (2016).
- [15] Y. Cao, J. Y. Luo, V. Fatemi, S. Fang, J. D. Sanchez-Yamagishi, K. Watanabe, T. Taniguchi, E. Kaxiras, and P. Jarillo-Herrero, Superlattice-Induced Insulating States and Valley-Protected Orbits in Twisted Bilayer Graphene, *Phys. Rev. Lett.* **117**, 116804 (2016).
- [16] A. Luican, G. Li, A. Reina, J. Kong, R. R. Nair, K. S. Novoselov, A. K. Geim, and E. Y. Andrei, Single-Layer Behavior and Its Breakdown in Twisted Graphene Layers, *Phys. Rev. Lett.* **106**, 126802 (2011).
- [17] L.-J. Yin, J.-B. Qiao, W.-X. Wang, W.-J. Zuo, W. Yan, R. Xu, R.-F. Dou, J.-C. Nie, and L. He, Landau quantization and Fermi velocity renormalization in twisted graphene bilayers, *Phys. Rev. B* **92**, 201408(R) (2015).
- [18] T. Ohta, J. T. Robinson, P. J. Feibelman, A. Bostwick, E. Rotenberg, and T. E. Beechem, Evidence for Interlayer Coupling and Moiré Periodic Potentials in Twisted Bilayer Graphene, *Phys. Rev. Lett.* **109**, 186807 (2012).
- [19] H. Peng, N. B. M. Schroter, J. Yin, H. Wang, T.-F. Chung, H. Yang, S. Ekehana, Z. Liu, J. Jiang, L. Yang, T. Zhang, C. Chen, H. Ni, A. Barinov, Y. P. Chen, Z. Liu, H. Peng, and Y. Chen, Substrate doping effect and unusually large angle van Hove singularity evolution in twisted bi- and multilayer graphene, *Adv. Mater.* **29**, 1606741 (2017).
- [20] A. J. H. Jones, R. Muzzio, P. Majchrzak, S. Pakdel, D. Curcio, K. Volckaert, D. Biswas, J. Gobbo, S. Singh, J. T. Robinson, K. Watanabe, T. Taniguchi, T. K. Kim, C. Cacho, N. Lanata,

- J. A. Miwa, P. Hofmann, J. Katoch, and S. Ulstrup, Observation of electrically tunable van Hove singularities in twisted bilayer graphene from nanoARPES, *Adv. Mater.* **32**, 2001656 (2020).
- [21] M. I. B. Utama, R. J. Koch, K. Lee, N. Leconte, H. Li, S. Zhao, L. Jiang, J. Zhu, K. Watanabe, T. Taniguchi, P. D. Ashby, A. Weber-Bargioni, A. Zettl, C. Jozwiak, J. Jung, E. Rotenberg, A. Bostwick, and F. Wang, Visualization of the flat electronic band in twisted bilayer graphene near the magic angle twist, *Nat. Phys.* **17**, 184 (2021).
- [22] S. Lisi, X. Lu, T. Benschop, T. A. de Jong, P. Stepanov, J. R. Duran, F. Margot, I. Cucchi, E. Cappelli, A. Hunter, A. Tamai, V. Kandyba, A. Giampietri, A. Barinov, J. Jobst, V. Stalman, M. Leeuwenhoek, K. Watanabe, T. Taniguchi, L. Rademaker *et al.*, Observation of flat bands in twisted bilayer graphene, *Nat. Phys.* **17**, 189 (2021).
- [23] I. Rizado-Colambo, J. Avila, J. P. Nys, C. Chen, X. Wallart, M. C. Asensio, and D. Vignaud, NanoARPES of twisted bilayer graphene on SiC: Absence of velocity renormalization for small angles, *Sci. Rep.* **6**, 27261 (2016).
- [24] H. Imamura, A. Visikovskiy, R. Uotani, T. Kajiwara, H. Ando, T. Iimori, K. Iwata, T. Miyamachi, K. Nakatsuji, K. Mase, T. Shirasawa, F. Komori, and S. Tanaka, Twisted bilayer graphene fabricated by direct bonding in a high vacuum, *Appl. Phys. Express* **13**, 075004 (2020).
- [25] T. Kosugi, H. Nishi, Y. Kato, and Y.-i. Matsushita, Periodicity-free unfolding method of electronic energy spectra, *J. Phys. Soc. Jpn.* **86**, 124717 (2017).
- [26] C. Riedl, U. Starke, J. Bernhardt, M. Franke, and K. Heinz, Structural properties of the graphene-SiC(0001) interface as a key for the preparation of homogeneous large-terrace graphene surfaces, *Phys. Rev. B* **76**, 245406 (2007).
- [27] A. Toyoshima, T. Kikuchi, H. Tanaka, K. Mase, K. Amemiya, and K. Ozawa, Performance of PF BL-13A, a vacuum ultraviolet and soft x-ray undulator beamline for studying organic thin films adsorbed on surfaces, *J. Phys.: Conf. Ser.* **425**, 152019 (2013).
- [28] See Supplemental Material at <http://link.aps.org/supplemental/10.1103/PhysRevMaterials.5.L051001> for details of the calculations, additional ARPES data, and results of the calculations, which includes Refs. [34–36].
- [29] J. D. Emery, B. Detlefs, H. J. Karmel, L. O. Nyakiti, D. K. Gaskill, M. C. Hersam, J. Zegenhagen, and M. J. Bedzyk, Chemically Resolved Interface Structure of Epitaxial Graphene on SiC(0001), *Phys. Rev. Lett.* **111**, 215501 (2013).
- [30] K. Uchida, S. Furuya, J.-I. Iwata, and A. Oshiyama, Atomic corrugation and electron localization due to moiré patterns in twisted bilayer graphenes, *Phys. Rev. B* **90**, 155451 (2014).
- [31] S. Dai, Y. Xiang, and D. J. Srolovitz, Twisted bilayer graphene: Moiré with a twist, *Nano Lett.* **16**, 5923 (2016).
- [32] N. N. T. Nam and M. Koshino, Lattice relaxation and energy band modulation in twisted bilayer graphene, *Phys. Rev. B* **96**, 075311 (2017).
- [33] P. Lucignano, D. Alfè, V. Cataudella, D. Ninno, and G. Cantele, Crucial role of atomic corrugation on the flat bands and energy gaps of twisted bilayer graphene at the magic angle $\theta \sim 1.08^\circ$, *Phys. Rev. B* **99**, 195419 (2019).
- [34] J. C. Slater and G. F. Koster, Simplified LCAO method for the periodic potential problem, *Phys. Rev.* **94**, 1498 (1954).
- [35] G. Trambly de Laissardière, D. Mayou, and L. Magaud, Numerical studies of confined states in rotated bilayers of graphene, *Phys. Rev. B* **86**, 125413 (2012).
- [36] Y.-i. Matsushita, H. Nishi, J.-i. Iwata, T. Kosugi, and A. Oshiyama, Unfolding energy spectra of double-periodicity two-dimensional systems: Twisted bilayer graphene and MoS₂ on graphene, *Phys. Rev. Materials* **2**, 010801(R) (2018).